



Minerva Access is the Institutional Repository of The University of Melbourne

Author/s:

Magaye, RR;Savira, F;Xiong, X;Huynh, K;Meikle, PJ;Reid, C;Flynn, BL;Kaye, D;Liew, D;Wang, BH

Title:

Dihydrosphingosine driven enrichment of sphingolipids attenuates TGF $\beta$  induced collagen synthesis in cardiac fibroblasts

Date:

2021-08-01

Citation:

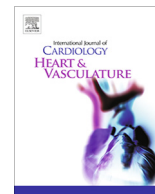
Magaye, R. R., Savira, F., Xiong, X., Huynh, K., Meikle, P. J., Reid, C., Flynn, B. L., Kaye, D., Liew, D. & Wang, B. H. (2021). Dihydrosphingosine driven enrichment of sphingolipids attenuates TGF $\beta$  induced collagen synthesis in cardiac fibroblasts. *Ijc Heart and Vasculature*, 35, <https://doi.org/10.1016/j.ijcha.2021.100837>.

Persistent Link:

<https://hdl.handle.net/11343/281863>

License:

[CC BY-NC-ND](#)



## Dihydrospingosine driven enrichment of sphingolipids attenuates TGF $\beta$ induced collagen synthesis in cardiac fibroblasts

Ruth R. Magaye<sup>a,b</sup>, Feby Savira<sup>a,b</sup>, Xin Xiong<sup>a,b,c</sup>, Kevin Huynh<sup>d</sup>, Peter J. Meikle<sup>d,e</sup>, Christopher Reid<sup>b,e</sup>, Bernard L. Flynn<sup>f</sup>, David Kaye<sup>g</sup>, Danny Liew<sup>b</sup>, Bing H. Wang<sup>a,b,\*</sup>

<sup>a</sup> Biomarker Discovery Laboratory, Baker Heart and Diabetes Institute, Melbourne, Australia

<sup>b</sup> Monash Centre of Cardiovascular Research and Education in Therapeutics, Melbourne, Australia

<sup>c</sup> Shanghai Institute of Heart Failure, Research Centre for Translational Medicine, Shanghai East Hospital, Tongji University, School of Medicine, Shanghai 200120, PR China

<sup>d</sup> Metabolomics Research Group, Baker Heart and Diabetes Institute, Melbourne, Australia

<sup>e</sup> School of Public Health School, Curtin University, Perth, Australia

<sup>f</sup> Monash Institute of Pharmaceutical Sciences, Monash University, Melbourne, Australia

<sup>g</sup> Heart Failure Research Group, Baker Heart and Diabetes Institute, Melbourne, Australia

### ARTICLE INFO

#### Article history:

Received 24 February 2021

Received in revised form 24 June 2021

Accepted 27 June 2021

#### Keywords:

Cardiac fibroblasts  
Collagen synthesis  
Dihydrospingosine  
Sphingolipid  
TGF $\beta$

### ABSTRACT

The sphingolipid de novo synthesis pathway, encompassing the sphingolipids, the enzymes and the cell membrane receptors, are being investigated for their role in diseases and as potential therapeutic targets. The intermediate sphingolipids such as dihydrospingosine (dhSph) and sphingosine (Sph) have not been investigated due to them being thought of as precursors to other more active lipids such as ceramide (Cer) and sphingosine 1 phosphate (S1P). Here we investigated their effects in terms of collagen synthesis in primary rat neonatal cardiac fibroblasts (NCFs). Our results in NCFs showed that both dhSph and Sph did not induce collagen synthesis, whilst dhSph reduced collagen synthesis induced by transforming growth factor  $\beta$  (TGF $\beta$ ). The mechanisms of these inhibitory effects were associated with the increased activation of the de novo synthesis pathway that led to increased dihydrospingosine 1 phosphate (dhS1P). Subsequently, through a negative feedback mechanism that may involve substrate-enzyme receptor interactions, S1P receptor 1 expression (S1PR1) was reduced.

© 2021 Published by Elsevier B.V. This is an open access article under the CC BY-NC-ND license (<http://creativecommons.org/licenses/by-nc-nd/4.0/>).

### 1. Introduction

The sphingolipids such as Cer and S1P have been targeted in recent years for therapeutic interventions in cancer therapy due

**Abbreviations:** Akt, protein kinase B; Cer, ceramide; Cer1P, ceramide 1 phosphate; Coll1a1, collagen 1a1; CTGF, connective tissue growth factor; d7dhSph, deuterated dihydrospingosine; Degs1, dihydroceramide desaturase 1 gene; Des-1, dihydroceramide desaturase 1 enzyme; dhCer, dihydroceramide; dhS1P, dihydrospingosine 1 phosphate; ECM, extracellular matrix inhibitor of nuclear kappa B (NFK $\beta$ ) kinase alpha and beta (IKK $\alpha/\beta$ ); MAPK, mitogen activated protein kinase; MA3PK, mitogen activated protein kinase kinase kinase; MI, myocardial infarct; MMP2, matrix metalloproteinase 2; mTOR, mammalian target for rapamycin; NCF, neonatal cardiac fibroblasts; RPS6, ribosomal protein S6; S1P, sphingosine-1 Phosphate; S1PRs, sphingosine 1 phosphate receptor 1-5; S1PR1, sphingosine -1-phosphate receptor 1; Sph, sphingosine; SK1, sphingosine kinase 1; TAK1, transforming growth factor  $\beta$  activating kinase 1; TGF $\beta$ , transforming growth factor  $\beta$ ; TIMP1, tissue inhibitor of metalloproteinase 1.

\* Corresponding author at: Biomarker Discovery Laboratory, Baker Heart and Diabetes Institute, Melbourne, Australia.

E-mail addresses: [bing.wang@baker.edu.au](mailto:bing.wang@baker.edu.au), [bing.wang@monash.edu](mailto:bing.wang@monash.edu) (B.H. Wang).

<https://doi.org/10.1016/j.ijcha.2021.100837>

2352-9067/© 2021 Published by Elsevier B.V.

This is an open access article under the CC BY-NC-ND license (<http://creativecommons.org/licenses/by-nc-nd/4.0/>).

to their apoptotic and proliferative effects on cancer cells. Apart from these, several of the so called “intermediate” lipids in the de novo sphingolipid synthesis pathway may have a role in several pathologies including cardiovascular diseases [1]. In the setting of a number of cardiomyopathies other researchers have shown these intermediate sphingolipids (dhSph and Sph) are also altered in both plasma and tissue of animal models [2,3] and in the blood of patients [4–6]. However, due to the lack of basic mechanistic pathway research regarding their effects or interactions with well-known cardiac remodelling markers such as TGF $\beta$ , no conclusions could be drawn in regards to what these alterations may imply.

Within the cellular system, Sph is produced either because of the metabolic effects of ceramidase (CDase) on Cer or salvaged in the lysosome from the breakdown products of sphingolipids. While dhSph is derived from the de novo synthesis pathway and is a product of the reducing effects of 3-keto reductase on 3-ketosphinganine. The phosphorylation of both Sph and dhSph by sphingosine kinase 1 & 2 (SK1 & 2) results in the production of

S1P and dhS1P. Furthermore, the acylation of dhSph by ceramide synthase 1 to 6 (CerS1-6) results in the production of dihydroceramide (dhCer) which is then converted to Cer in a non-reversible reaction catalysed by dihydroceramide desaturase 1 and 2 (DES1 and 2). Several feedback mechanisms are at play in the de novo pathway [7], involving both the sphingolipids and the enzymes to regulate these sphingolipids in the disease states, thus their interaction with factors such as TGF $\beta$  are irrefutable. However, they have hardly been investigated in cardiac cells. Inhibition of DES1; which results in cellular accumulation of sphingolipid species such as dhCer and dhSph in liver cells and cancer cells have shown reduced cell cycle progression and proliferation [8–10]. The growth and proliferative effects of TGF $\beta$  on cells, including cardiac cells leading to increased proliferation and collagen synthesis, is well understood. There is evidence of TGF $\beta$  increasing SK1 activity in muscle cells giving rise to fibrosis [11]. This study was conducted to determine whether extracellular dhSph and Sph influence TGF $\beta$  induced collagen synthesis in cardiac fibroblasts in a primary cell culture system.

## 2. Methods

Primary NCFs (ventricular) were extracted from 1 to 2 days old Sprague-Dawley rat pups (80 pups per isolation/experiment) using enzymatic collagenase digestion routinely used in our laboratory for *in vitro* assays [12]. Pups were purchased from the Monash Animal Research Platform (Clayton, Vic), and all experimental procedures complied with the guidance from the National Health and Medical Research Council of Australia. The animal used for this study was approved by the Alfred Medical Research and Education Precinct Animal Ethics Committee (E/1653/2016/M).

### 2.1. Measurement of cardiac fibroblast collagen synthesis

Collagen synthesis in NCFs stimulated by TGF $\beta$  were determined using the  $^3\text{H}$ -proline incorporation assay [13]. Briefly, NCFs were pre-treated for 2 h with Sph, dhSph and dhS1P (0.01–10.0  $\mu\text{M}$ ; Toronto Research Chemicals Incorporated, North York, ON, Canada) in DMEM F12 medium supplemented with 1% vitamin C and 0.5% BSA. 1  $\mu\text{Ci}$   $^3\text{H}$ -proline was incorporated with TGF $\beta$  (100–21C, PeproTech, Rocky Hill, NJ, USA) and further incubated for 48 h. After precipitation with 10% trichloroacetic acid (TCA) for 30 min, the cell pellets were detached in 1 M sodium hydroxide (NaOH) and solubilized in 1:10 ratio of 1 M hydrochloric acid (HCl) with scintillation fluid.  $^3\text{H}$ -proline incorporation levels were determined on a 300SL beta counter at counts per minute (cpm).

### 2.2. Measurement of cell viability in rat NCFs

Almar Blue Assay (Invitrogen- Thermo Fischer Scientific, Carlsbad, CA, USA) was used to determine the cell viability of NCFs in the presence of the sphingolipids and TGF $\beta$  according to manufacturer's guidelines as reported previously [14].

### 2.3. Quantitative measurement of protein levels in NCFs

Western blotting was used to quantify the expression of specific proteins related to cardiac remodelling. Cells were seeded as mentioned previously [14], and pre-treated for 2 h with Sph and dhSph (1.0–10.0  $\mu\text{M}$ ). The expression of phosphorylated proteins was determined at 18 min of treatment with TGF $\beta$ , and 24 h for total proteins. 10  $\mu\text{g}/\mu\text{L}$  of denatured proteins were separated on 7.5, 10, or 12% gels by sodium dodecyl sulfate–polyacrylamide gel electrophoresis (SDS–PAGE), and transferred onto nitrocellulose blotting membranes (GE HealthCare, Chicago, IL, USA). The blots

were blocked with 5% bovine serum albumin (BSA) and probed with antibodies specific for phosphorylated, protein kinase B (Akt), inhibitor of nuclear kappa B (NFK $\beta$ ) kinase alpha and beta (IKK $\alpha/\beta$ ), NFK $\beta$ , P38- MAPK, extracellular-signal-regulated kinase (ERK), ribosomal protein S6 (RPS6), signal transducer and activator of transcription 1 (STAT1), and SMAD2 from Cell Signalling Technologies (CST, Danvers, MA, USA: 4060L, 2694, 4631, 3033, 9101, 8826S, 5364T, and 3108L). They were also probed for TGF $\beta$  (CST: 3709S). Bands were detected using Super Signal West Pico Chemiluminescence Substrate (Thermo Fisher Scientific, Rockford, IL, United States) on the BioRad Chemidoc instrument and analysed using Image lab software (BioRad Laboratories, Hercules, CA, USA). Proteins were normalised to glyceraldehyde 3 -phosphate dehydrogenase (GAPDH) (CST: 2118L).

### 2.4. Quantitative measurement of genes expressed in cardiac remodelling

Real time polymerase chain reaction (rt-PCR) was used to ascertain Sph and dhSph effect on changes in gene expression induced by TGF $\beta$ . NCFs were seeded as previously mentioned, and pre-treated with the inhibitors for 2 h. Cells were further incubated for 18 h with 10 ng/ml TGF $\beta$ . Similar RNA extraction and transcription methods mentioned previously were used [14]. The expression levels of the fibrotic markers: TGF $\beta$ , connective tissue growth factor (CTGF), tissue inhibitor of metalloproteinase 1 and 2 (TIMP1 and TIMP2), collagen 1a1 (Coll1a1), the S1P receptors 1, 2 and 3 (S1PR1-3), and the enzymes SK1, and Des-1 (Degs1) were quantified by rt-PCR on the Quant-Studio 12 K Flex Real Time PCR System with SYBR Green detection method (Applied Biosystems). 18 s mRNA was used as the endogenous control. The sequences of the primers used are listed in supplementary Table 1.

### 2.5. Tracing relative d7-dhSph in NCFs

Cardiac fibroblasts extracted from neonatal rats were cultured in 6 well plates at 200 000 cells/ well at passage 2. After 48 h serum starvation, the cells were treated with 1  $\mu\text{M}$  d7-dhSph (Cayman Chemical Company, Ann Arbor, MI, USA) in DMEM F12 with 0.5% BSA at different time points. The cells were then washed 3 times with PBS, scrapped in 1 mL PBS, transferred into Eppendorf tubes and placed on ice. NCFs were then sonicated (Misonix S4000-Ultrasonic Liquid Processor, Qsonica, Newton, CT, United States) at 25 amplitudes for 10 s each. Samples were then snap frozen on dry ice until processed for liquid chromatography–mass spectrophotometry (LC–MS) according to previously published methods with modification for cultured cells [15,16]. The Agilent 6490 QQQ mass spectrometer with an Agilent 1290 series HPLC system and a ZORBAX eclipse plus C18 column (2.1x100mm 1.8  $\mu\text{m}$ , Agilent) with the thermostat set at 45  $^{\circ}\text{C}$  was used to analyse the cell extracts. Mass spectrometry analysis was performed with dynamic scheduled multiple reaction monitoring (MRM) in positive ion mode. We scanned for both the endogenous sphingolipids and sphingolipids with tracer incorporation, where tracer incorporation utilised a 7 Da offset for the precursor and/or product ion depending on the sphingolipid species. Relative enrichment was calculated as area of the labelled species/(area of labelled species + area of non-labelled species).

### 2.6. Statistical analysis

All cell culture experiments were performed in triplicates, with at least three repeated experiments for the collagen synthesis assays and two repeated experiments for Western Blots and rt-PCR. The results are presented as the percentage of unstimulated controls (mean  $\pm$  SEM). For Western blot analyses, the ratios of

phosphorylated protein over GAPDH levels were analysed. For PCR, gene expression levels in NCF were normalised with 18s (house-keeping gene). One-way ANOVA with Bonferroni's multiple comparison post hoc tests was used for statistical analyses for comparison between multiple groups and unpaired *t*-test was used for comparison between two groups. A statistically significant result was determined with a two-tailed *p*-value of <0.05. GraphPad Prism Version 9 (GraphPad Software Inc., San Diego, CA, United States) was used to perform all the statistical analyses.

### 3. Results

#### 3.1. Extracellular Sph and dhSph alone did not induce collagen synthesis in NCFs

To ascertain whether exogenous dhSph and Sph have effects on collagen synthesis, we determined their effect on cultured NCFs using the <sup>3</sup>H-proline incorporation Assay. As shown in Fig. 1A at the doses of 0.1, 0.3, 1 and 3 μM both dhSph and Sph did not induce collagen synthesis. However, dhSph at the highest dose of 3 μM (*p* < 0.01) significantly reduced <sup>3</sup>H-proline incorporation levels compared to the control. This was corroborated by the cell viability results which showed that 3 μM dhSph treatment significantly reduced NCF viability (*p* < 0.001, Fig. 1B), while Sph had no effect.

#### 3.2. DhSph reduced collagen synthesis induced by TGFβ

We then determined whether dhSph and Sph were able to reduce collagen synthesis induced by a known collagen inducing agent, TGFβ. DhSph (0.1, 0.3, and 1 μM; *p* < 0.05, 3 μM; *p* < 0.0001) significantly reduced collagen synthesis induced by TGFβ (*p* < 0.0001, Fig. 1C). Sph did not have significant effect on TGFβ induced collagen synthesis at the doses investigated. The viability of NCFs treated with dhSph and Sph were not affected in the presence of TGFβ (Fig. 1D). TGFβ's ability to modulate cell growth

or increase proliferation may have counteracted the effects of dhSph alone as observed in Fig. 1A & B.

#### 3.3. DhSph reduces SMAD2 phosphorylation stimulated by TGFβ

TGFβ utilises the canonical TGFβ/SMAD signalling pathway to induce collagen synthesis, therefore since dhSph reduced collagen synthesis in NCFs, we determined whether it can attenuate SMAD2 phosphorylation. DhSph significantly diminished SMAD2 phosphorylation stimulated by TGFβ in NCFs at 1 μM (*p* < 0.05, Fig. 2A). Sph had no effect on TGFβ induced SMAD2 phosphorylation.

#### 3.4. DhSph reduces TGFβ protein expression

The human recombinant TGFβ [17,18] activates TGFβ receptor 1 and 2 resulting in increased TGFβ protein expression. DhSph (0.1 and 1 μM) treatment significantly inhibited the increased expression of 65 kDa latent TGFβ protein in NCFs (Fig. 2C) but had no significant effect on the 45 kDa isoform (Fig. 2D). There was a trend toward a reduction on the mature 25 kDa TGFβ protein isoform by dhSph (Fig. 2E), however it did not reach significance.

#### 3.5. DhSph affects Akt- RPS6 signalling in TGFβ treated cells

We compared the effects of dhSph and Sph on Akt-RPS6 signalling. Both dhSph (*p* < 0.05) and Sph (*p* < 0.05) reduced Akt phosphorylation by TGFβ in NCFs (Fig. 3C). Additionally, dhSph and Sph had significant effect on the phosphorylation of the downstream protein RPS6 in the Akt pathway (*p* < 0.05 and *p* < 0.005, Fig. 3D).

#### 3.6. DhSph and Sph have no effect on ERK and P38-MAPK pathways, and NFκB and STAT1 transcription factors

We also compared the effects of Sph and dhSph on the ERK, P38- MAPK and IKK pathways and transcription factors such as STAT1 and NFκB. Both dhSph and Sph did not have any effect on

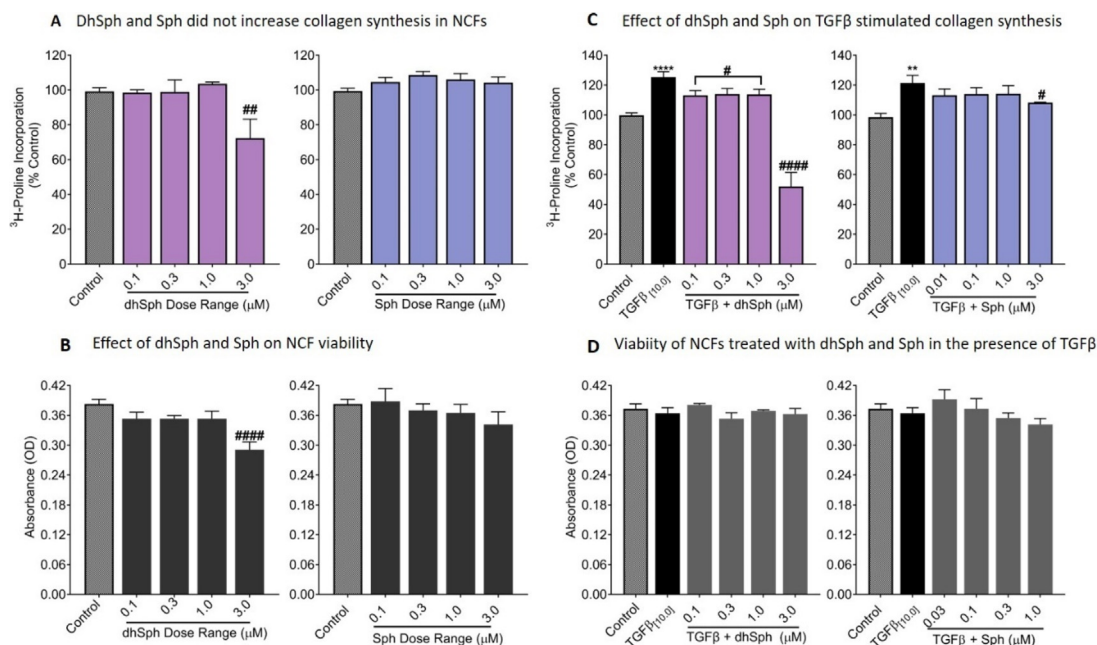


**Fig. 1.** Effect of dhSph and Sph on collagen synthesis and viability in NCFs. (A) Treatment of NCFs with dhSph and Sph at 0.1, 0.3, 1 and 3 μM for 48 h did not induce collagen synthesis. (B) DhSph significantly reduced the viability of NCFs at 3 μM (*p* < 0.005), but Sph had no significant effect on NCFs at all doses tested. (C) DhSph significantly reduced collagen synthesis in NCFs induced by TGFβ at 48 h, while the effects of Sph were not statistically significant. (D) The viability of NCFs were not affected by dhSph and Sph treatment in the presence of TGFβ. #### *p* < 0.001, ## *p* < 0.01, # *p* < 0.05 vs. treatment, \*\*\* *p* < 0.005, \*\*\*\* *p* < 0.0001 vs. control. Data are presented as ± SEM of 3 replicates.

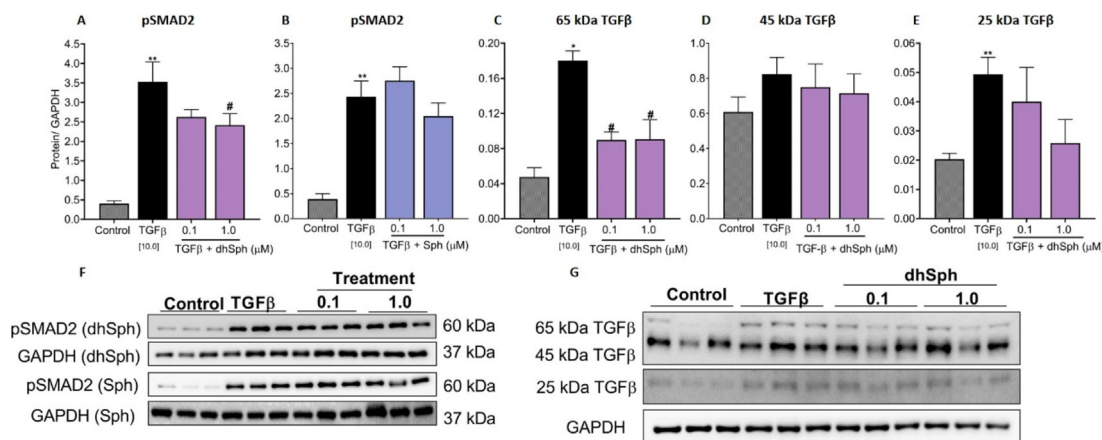


**Fig. 2.** Effect of dhSph on the canonical TGF $\beta$  pathway. (A) Pre-treatment of NCFs with 1  $\mu$ M dhSph significantly reduced SMAD2 phosphorylation stimulated by 10 ng/ml TGF $\beta$  at 18 min ( $p < 0.05$ ). (B) Sph (0.1 and 1  $\mu$ M) had no effect on TGF $\beta$  induced phosphorylation of SMAD2. DhSph significantly reduced (C) the 65 kDa latent TGF $\beta$ , but (D) had no effect on 45 kDa latent TGF $\beta$ , and the (E) 25 kDa mature TGF $\beta$  in NCFs treated with the human recombinant TGF $\beta$ . (F) and (G) show representative blots. Refer to supplementary figure 2 for original blots. \* $p < 0.05$  vs. TGF $\beta$ , \*\* $p < 0.01$ , # $p < 0.05$  vs. control. Data are presented as  $\pm$  SEM of 3 replicates.

the phosphorylation levels of P38- MAPK (Fig. 3A) and ERK (Fig. 3B), which were elevated by TGF $\beta$  ( $p < 0.05$  and  $p < 0.01$ , respectively). TGF $\beta$  increased phosphorylation of IKK $\alpha/\beta$  ( $p < 0.01$ , Fig. 3F), while dhSph and Sph had no effect on IKK $\alpha/\beta$  and its downstream target, NF $\kappa$ B (Fig. 3G). Even though dhSph raised the phosphorylation level of the transcription factor STAT1 (Fig. 3E) in the presence of TGF $\beta$ , the difference was not statistically significant.

### 3.7. Basal levels of Cer d18:1 and S1P d16:1 species were higher in NCFs

We then investigate the level of unlabelled sphingolipids in NCFs to determine their basal levels. CerS1-6 are responsible for attaching different acyl chain lengths to the sphingoid base. In the heart CerS4 (C18 and C20), 5 (C16), and 2 (C20-C26) have been shown to be expressed the most [19]. The mean basal level of unlabelled Cer(18:1/18:0) was around 77.62 pmol $\mu$ mol (Fig. 4A2) which was higher than all other sphingolipid species measured showing that CerS4 expression maybe higher in NCFs. Other Cer species such as 18:1/16:0, 18:1/20:0, 18:1/24:0, 18:1/22:0, and 18:1/24:1 had low mean basal levels (0.39, 0.04, 0.09, 0.03, 0.03 and 0.008 pmol $\mu$ mol, respectively) (Fig. 4A2). The mean level of unlabelled dhCer measured in the control NCFs showed that dhCer 18:0/24:0 (6.09 pmol $\mu$ mol) was higher than dhCer 18:0/18:0, 18:0/16:0, 18:0/20:0 and 18:0/22:0 (4.13, 0.57, 0.41 and 0.9 pmol $\mu$ mol, respectively) as shown in Fig. 4A1. The mean basal level of SM 41:0 (7.17 pmol $\mu$ mol, supplementary excel data file 1B) was higher than SM 37:1, 32:1, 33:1, 34:1, 36:1, 38:1 and 40:1 (2.31, 0.06, 0.07, 0.02, 0.18, 0.55 and 0.09 pmol $\mu$ mol, respectively) in NCFs (Fig. 4AC). Furthermore, the level of unlabelled phosphorylated short chain sphingolipid S1P 16:1 (44.31 pmol $\mu$ mol, supplementary excel data file 1E) was higher than dhS1P 18:0 (16.2 pmol $\mu$ mol), S1P 18:1 (9.11 pmol $\mu$ mol), and ceramide 1 phosphate (Cer1P) 18:1 (5.51 pmol $\mu$ mol) (Fig. 4A4). Among the Sph species, mean basal level of short chain Sph (16:1) was higher (22.36 pmol $\mu$ mol) than Sph (17:1) and (18:1) (supplementary excel data file 1D).

### 3.8. DhSph-d7 enriches sphingolipids in a predictive manner in NCFs

DhSph is an intermediate lipid in the sphingolipid pathway, therefore its incorporation enriches other lipids in the de novo sphingolipid pathway. We used isotopically (deuterium) labelled

dhSph (dhSph-d7) to determine the time at which dhSph is incorporated into NCFs and assessed the type of lipids that were enriched. Looking at Fig. 4B1, it appears that dhSph-d7 is converted into dhCer quite rapidly (Fig. 4B1), but it's not until 60 min where more complex sphingolipids like SM begin to form (Fig. 4B3). Albeit at very minor quantities relative to endogenous basal levels, likely due to the stability of SM in membranes. Others such as Cer were enriched at approximately 30 min (Fig. 4B2).

### 3.9. DhSph-d7 enriched longer chain dhCer and Cer species

The longer chain dhCer d18:0/24:0 increased at around 30 min (19.94 pmol $\mu$ mol), reduced at 60 min and steadily increased, while d18:0/22:0 and d18:0/20:0 levels were increased to around 17.46 and 16.23 pmol $\mu$ mol at 120 min (Fig. 4B1). While the shorter chain d18:0/16:0 increased to around 11.45 pmol $\mu$ mol at 30 min, remained stable to 120 min and decreased afterward. Cer d18:1/24:1 level was the highest at 240 min, rising from 0.008 pmol $\mu$ mol at basal level to 2.99 pmol $\mu$ mol (Fig. 4B2). Cer d18:1/20:0 and 24:0 were also increased at this time point. The shorter chain Cer d18:1/16:0 increased to around 1.29 pmol $\mu$ mol at 30 min, before decreasing in a similar manner to dhCer d18:0/16:0. Most of the Cer species were elevated at 30 min but decreased afterward (supplementary excel data file 1A).

### 3.10. DhSph-d7 enriched dhS1P more than S1P and Cer1P

The phosphorylated sphingolipids target the G protein coupled S1PRs to activate intracellular signalling pathways. DhSph-d7 is almost immediately converted into dhS1P and hits saturation point, likely for removal in response to such high concentrations of exogenous dihydroshingosine. The incorporation of dhSph-d7 enriched d18:0 dhS1P at 10 min to about 80%, which remained at this level throughout the time points tested (Fig. 4C1). S1P and Cer1P were enriched at 10 to 30 min after dhSph-d7 treatment in NCFs (Fig. 4C2-3). The increase in S1P enrichment at 10 min maybe due to the dhSph-d7 being contaminated with d8-Sph. DhS1P was enriched more than S1P and Cer1P by dhSph-d7 (Fig. 4C4).

### 3.11. Exogenous dhS1P had synergistic effect on TGF $\beta$ induced collagen synthesis

Since dhS1P enrichment was increased early and remained for the duration of the experiment, we then examined the effects of

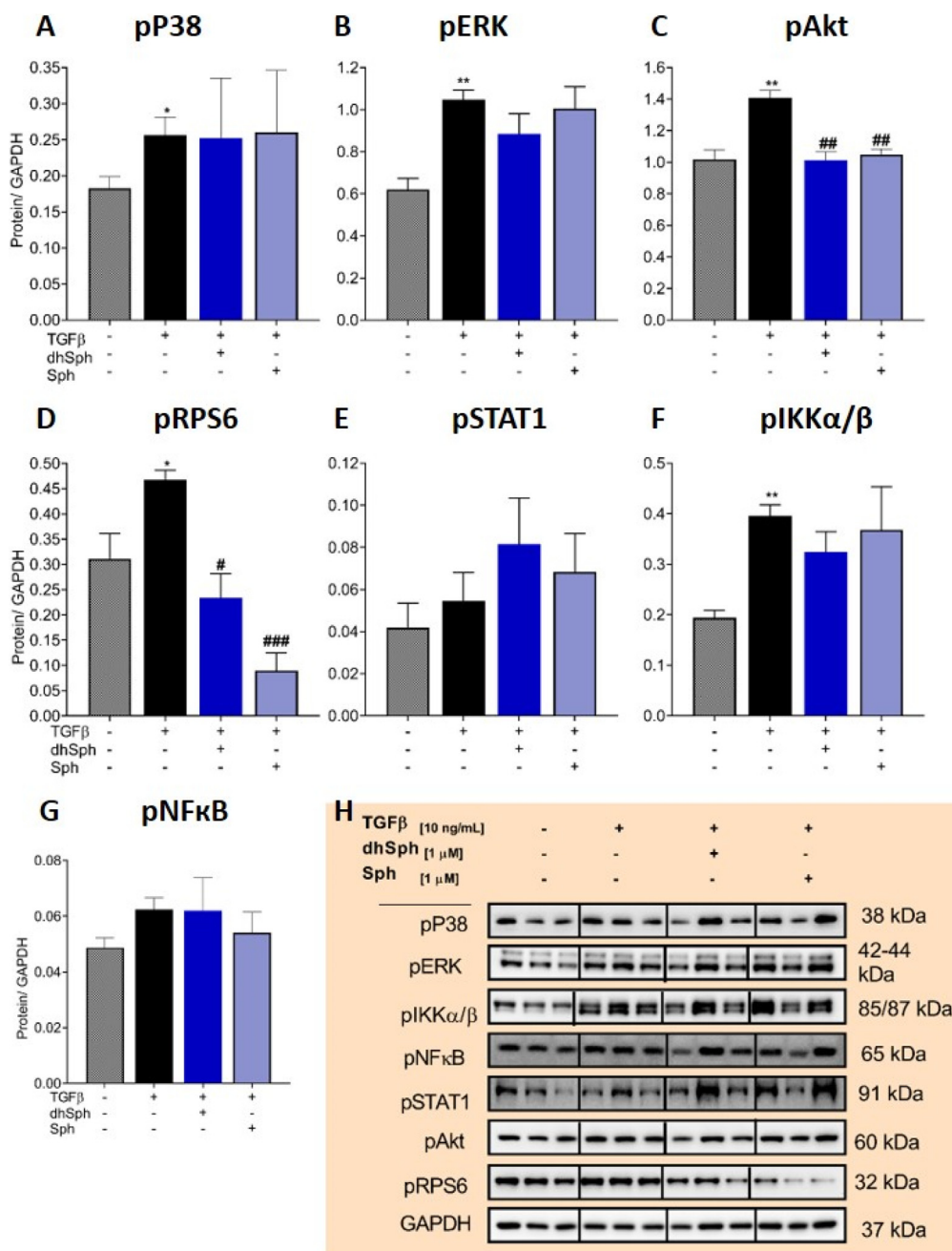


**Fig. 3.** Effect of dhSph and Sph on non-canonical TGFβ pathways. Pre-treatment of NCFs with 1 μM dhSph and Sph had no significant effect on (A) P38-MAPK, and (B) ERK phosphorylation induced by 10 ng/ml TGFβ at 18 min. (C) DhSph and Sph (1 μM) reduced TGFβ induced phosphorylation of Akt and (D) RPS6. DhSph and Sph had no effect on the phosphorylation levels of (E) STAT1, (F) IKKα/β and (G) NFκB in NCFs. (H) Representative blots in the presence and absence of TGFβ, Sph, and dhSph. ###*p* < 0.005, ##*p* < 0.01 vs. treatment, \*\**p* < 0.01, \**p* < 0.05 vs. control. Data are presented as ± SEM of 3 replicates.

dhS1P on TGFβ induced collagen synthesis in NCFs. Exogenous dhS1P had a synergistic effect on TGFβ induced collagen synthesis at 3 μM (*p* < 0.05). Additionally, the highest dose of dhS1P (10 μM) reduced collagen synthesis by TGFβ (*p* < 0.05, Fig. 5A). However, this effect was likely due to reduced viability of NCFs as shown in Fig. 5B, when compared to the control.

**3.12. DhSph reduces S1PR1 agonist, SEW2871, induced collagen synthesis**

We examined the effects of dhSph on collagen synthesis induced by the S1PR1 agonist, SEW2871. DhSph significantly reduced SEW2871 induced collagen synthesis at the highest dose

of 3 μM (*p* < 0.05, Fig. 5C). Sph had no effect on collagen synthesis induced by SEW2871 (Fig. 5D).

**3.13. DhSph and Sph had differing effects on TGFβ induced fibrotic genes**

Next, we examined the effects of dhSph and Sph on TGFβ induced fibrotic genes. In primary rat NCFs, stimulation with TGFβ for 18 h significantly increased TGFβ1 (*p* < 0.01), TIMP1 (*p* < 0.005) and CTGF mRNA levels (*p* < 0.001, Fig. 6A). DhSph significantly reduced TGFβ1 and TIMP1 at the higher dose of 1 μM (*p* < 0.05) but had no effect on CTGF mRNA. Sph had no effect on TGFβ1 and TIMP1 mRNA, but increased CTGF mRNA at the lower dose

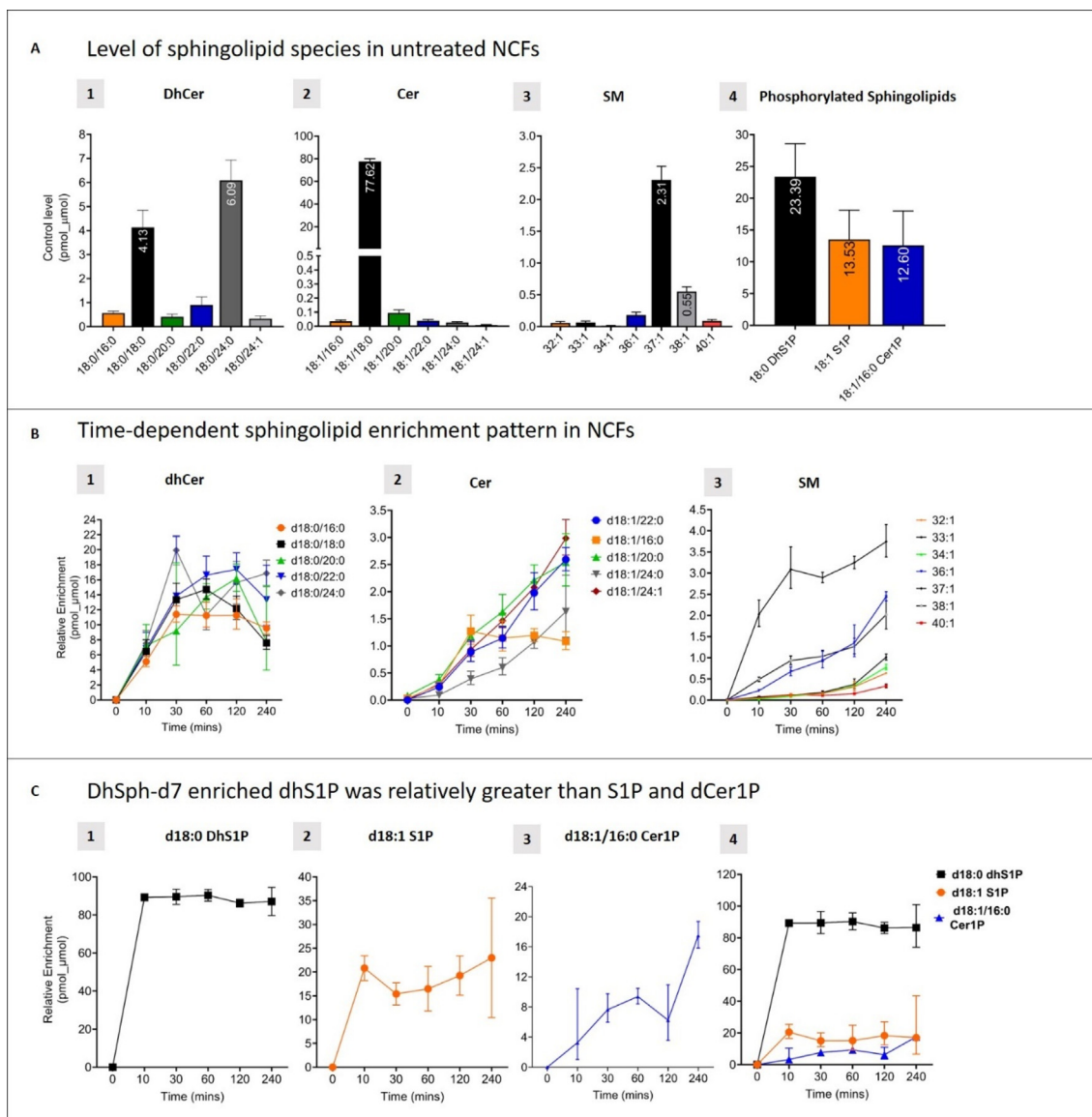


**Fig. 4.** Enrichment of sphingolipids by dhSph-d7. In NCFs, (A) among the unlabelled dhCer, and Cer, dhCer 18:0/24:0, and Cer 18:1/18:0 were higher. Among those treated with isotopically labelled dhSph-d7, (B1) dhCer was enriched at around 10 min, (B2) Cer at 30 min, (B3) and sphingomyelin at 120–240 min. DhSph-d7 also enriched the phosphorylated lipids (C1) d18:0 dhS1P, and (C2) d18:1 S1P within 10 min, and (C3) d18:1/16:0 Cer1P at 30 min. (C4) A comparative graph showing the enrichment of the three phosphorylated lipids across different time points. Data are presented as relative enrichment of 3 independent replicates, bars represent  $\pm$  SEM.

of 0.1  $\mu$ M ( $p < 0.05$ , Fig. 7B). After 18 h of treatment with TGF $\beta$ , there was no change in Coll 1a1 mRNA level in NCFs. Additionally, at this time point MMP2 ( $p < 0.005$ ) mRNA level was significantly reduced. Both dhSph and Sph had no effect on Coll1a1 and MMP2 mRNA levels in the presence of TGF $\beta$ .

### 3.14. DhSph reduced S1PR1 mRNA levels in NCFs

TGF $\beta$  is known to increase SK1 activity, therefore we examined the effect of dhSph and Sph on sphingolipid related genes. TGF $\beta$  significantly increased the mRNA levels of the de novo sphingolipid pathway enzymes, SK1 ( $p < 0.01$ ) and Degs1 (Fig. 7,  $p < 0.01$ ) at 18 h. Both dhSph and Sph had no effect on the expression levels of these genes. While, TGF $\beta$  had no effect on S1PR1–3 mRNA levels, dhSph significantly reduced S1PR1 mRNA levels ( $p < 0.05$ , Fig. 7A).

DhSph also had no effect on S1PR2 and S1PR3 mRNA levels. Curiously, Sph increased S1PR2 and 3 mRNA levels significantly ( $p < 0.05$ , Fig. 7B).

### 3.15. DhSph reduced fibrotic genes induced by the S1PR1 agonist

The effect of dhSph on collagen synthesis stimulated by SEW2871 and S1PR1 mRNA level in the presence of TGF $\beta$  led us to investigate its effect on SEW2871 induced changes in NCF genes expression. SEW2871 significantly raised Coll 1a1 ( $p < 0.01$ ), TGF $\beta$ 1 ( $p < 0.0001$ ), CTGF ( $p < 0.05$ ), TIMP1 ( $p < 0.0001$ ) and TIMP2 mRNA levels ( $p < 0.0001$ , Fig. 8A–D). DhSph significantly reduced Coll 1a1, TGF $\beta$ 1 ( $p < 0.05$ ), CTGF, TIMP1 and TIMP2 ( $p < 0.0001$ ) at the doses tested.

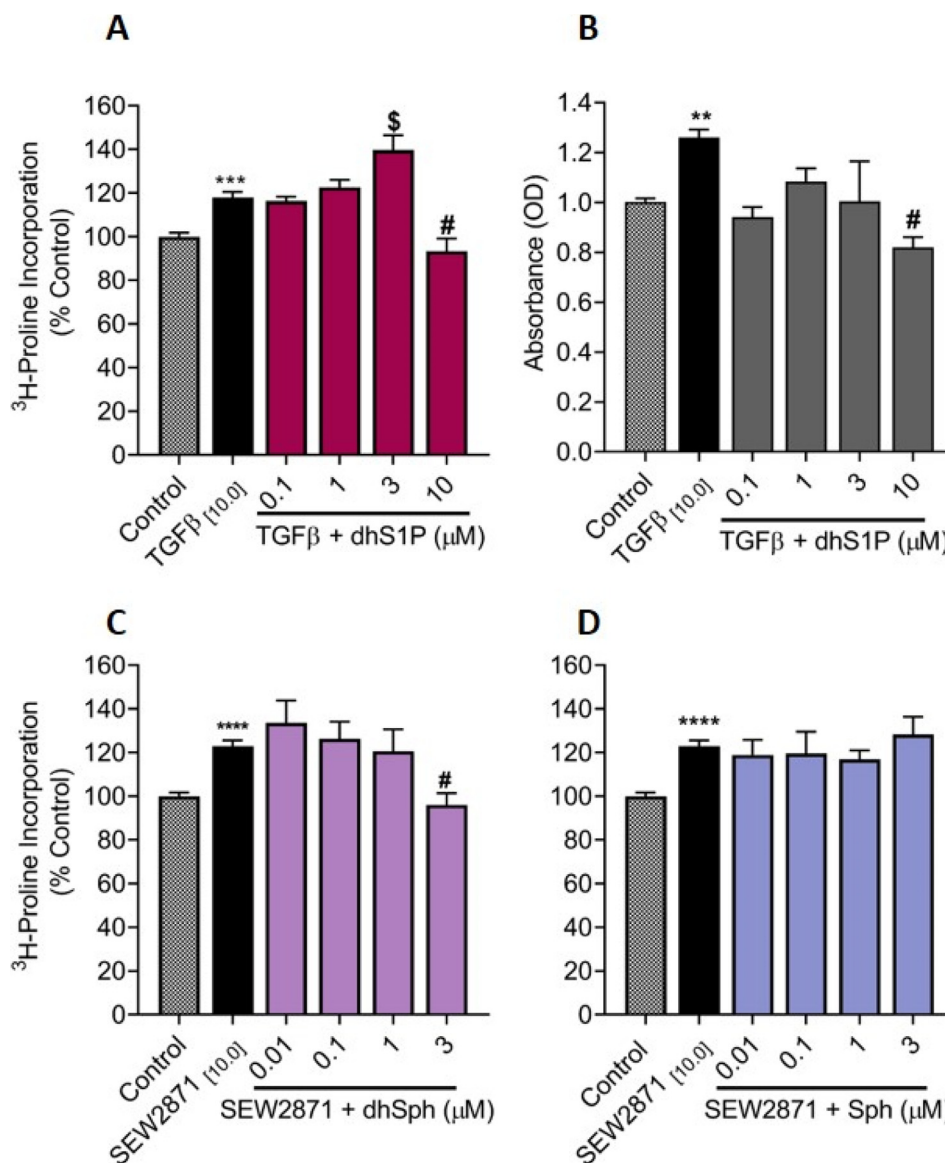


**Fig. 5.** Effect of dhS1P on TGFβ induced collagen synthesis. (A) In NCFs treated with dhS1P in the presence of TGFβ for 48 h, dhS1P (10 μM) reduced collagen synthesis. (B) The viability of NCFs was reduced by dhS1P (10 μM) in the presence of TGFβ for 48 h. (C) Treatment of NCFs with the S1PR1 agonist, SEW2871, increased collagen synthesis after 48 h, which was reduced by dhSph (3 μM). (D) Sph had no effect on SEW2871 induced collagen synthesis. #*p* < 0.05 vs. treatment, \*\*\*\**p* < 0.0001, \*\*\**p* < 0.001, \*\**p* < 0.01, vs. control. Data are presented as ± SEM of 3 replicates.

### 3.16. DhSph reduced S1PR1 and SK1 genes elevated by SEW2871

We investigated the effects of SEW2871 on sphingolipid related genes such as S1PR1, SK1 and Degs1. SEW2871 (10 μM) increased S1PR1 and SK1 gene expression levels in NCFs (Fig. 8F-G). The expression levels of these genes were significantly reduced by dhSph (1 and 3 μM). SEW2871 did not have significant effect on the Degs1 gene (Fig. 8H). However, dhSph showed a non-significant trend toward an increase in Degs1 gene expression in the presence of SEW2871.

## 4. Discussion

The sphingolipids, dhSph and Sph, are intermediate lipids in the *de novo* sphingolipid pathway. They are rapidly metabolised in the pathway to give rise to other patho-physiologically relevant lipids such as Cer and S1P. Their rapid metabolism also results in low

detection levels in plasma and tissue. Due to these reasons, their molecular effects on the pathway as a whole and in disease models such as cardiac remodelling are rarely explored. Recent studies on cell proliferation, apoptosis, autophagy and migration have alluded to the possibilities of targeting the sphingolipid pathway for therapeutics [20,21]. Here we investigated the effects of exogenous dhSph and Sph on primary NCFs in the presence of a well-known fibrotic factor, TGFβ.

In cardiac fibroblasts, TGFβ is known to increase collagen synthesis and drive the trans- differentiation of fibroblasts into myofibroblasts. TGFβ binds to either TGFβ receptor 1 and 2, which then activates the canonical pathway, involving the receptor activated SMADS (R-SMADS); SMAD2 and 3. Exogenous dhSph significantly reduced collagen synthesis stimulated by TGFβ in NCFs (Fig. 1C). The effect of dhSph on phosphorylation of SMAD2 (Fig. 2A), and Akt (Fig. 3C) implied that it was able to reduce collagen synthesis by targeting both canonical and non- canonical TGFβ signalling pathways [22]. However, the inhibitory effect on the non-

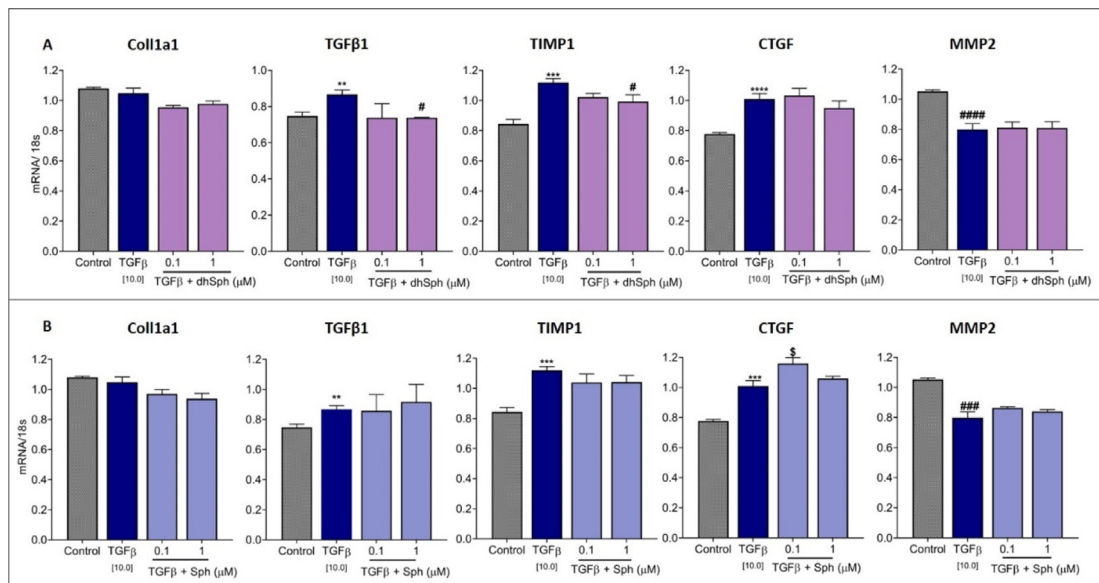


**Fig. 6.** Effect of dhSph and Sph on TGFβ induced fibrotic genes. In NCFs treated with 10 μM TGFβ for 18 h (A) dhSph reduced TGFβ and TIMP1 mRNA levels but had no effect on Coll 1a1, CTGF and MMP2. While (B) Sph had a synergistic effect on CTGF mRNA levels, but had no effect on TGFβ1, Coll 1a1, TIMP1 and MMP2. #*p* < 0.05, \**p* < 0.05, and \$*p* < 0.05 vs. treatment, ###*p* < 0.0001, and \*\*\*\**p* < 0.0001 vs. control. Data are presented as ± SEM of 3 replicates.

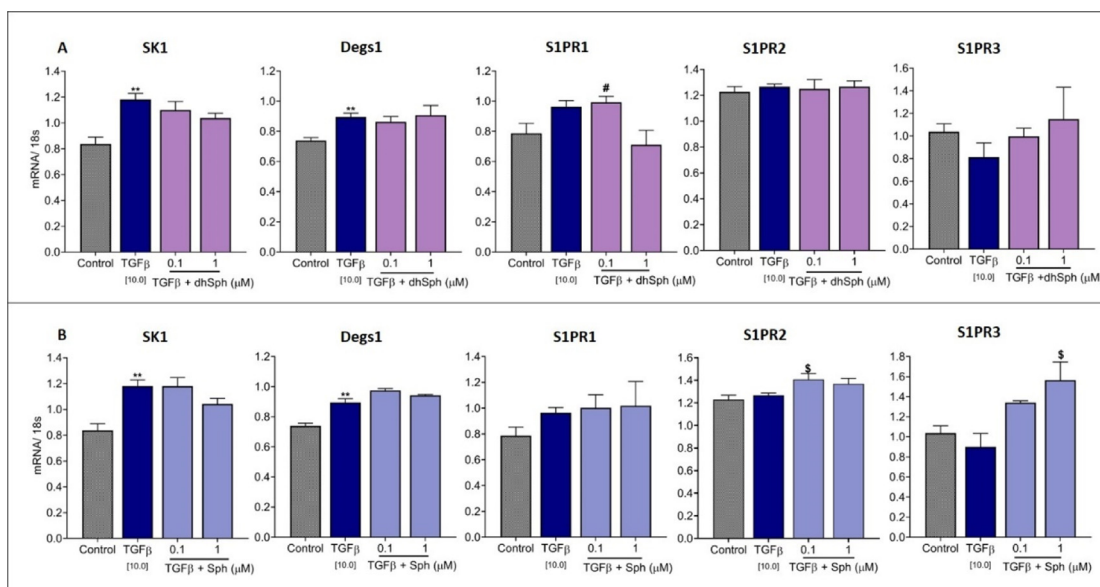


**Fig. 7.** Effect of dhSph and Sph on TGFβ induced sphingolipid related genes. (A) In NCFs treated with TGFβ 10 (ng/ml) for 18 h, dhSph reduced S1PR1 mRNA levels but had no effect on SK1, Dega1, S1PR2 and S1PR3. While (B) Sph increased S1PR2 & 3 in the presence of TGFβ (10 ng/ml) and had no effect on S1PR1, SK1 and Dega1 mRNA levels. #*p* < 0.01, \$*p* < 0.05 vs. treatment, and \$*p* < 0.0001 vs. control. Data are presented as ± SEM of 3 replicates.

canonical signalling pathway did not include NFκB phosphorylation (Fig. 3G). TGFβ signalling can be both rapid and delayed depending on experimental conditions. Direct activation of P38-MAPK by TGFβ occurs through MKK3 and MKK6, because of TGFβ activating kinase 1 (TAK1) activation which is a part of the MAP kinase kinase kinase (MAPK3K) [23]. TGFβ activation of Akt can occur through TRAF6 ubiquitination which also activates TAK1 [24]. Considering our experimental conditions, these pathways may be directly activated by TGFβ at 18 min in NCFs, while NFκB activation was likely delayed.

DhSph at higher doses caused cell death (Fig. 1B). This may be due to the increased cellular uptake with reduced metabolism leading to dhSph accumulating within the cell. The accumulation of dhSph is known to be associated with fumonisin toxicity in ani-

mals and humans [25–27]. However, at optimal doses, dhSph is rapidly metabolized, therefore, to further understand how dhSph was affecting TGFβ induced collagen synthesis we looked at the relative enrichment of other lipids in NCFs using deuterium labelled dhSph. As expected, addition of dhSph-d7 to cultured NCFs led to enrichment of dhCer, Cer, SM and dhS1P (Fig. 4). It is noteworthy that C18 and C16 acyl chain Cer and S1P had high basal levels in NCFs, showing that CerS4 and CerS5 expression may be higher in these cells (Supplementary excel data file 1A and 1E). This pattern has been observed in cardiac tissue expression of CerS [19]. This basal pattern changed with the addition of dhSph-d7, with longer acyl chain length species such as C24 and C20 staying elevated at 240 min compared to reducing shorter chain lengths (Fig. 4B1–3). CerS2 and 3 are responsible for attaching these longer

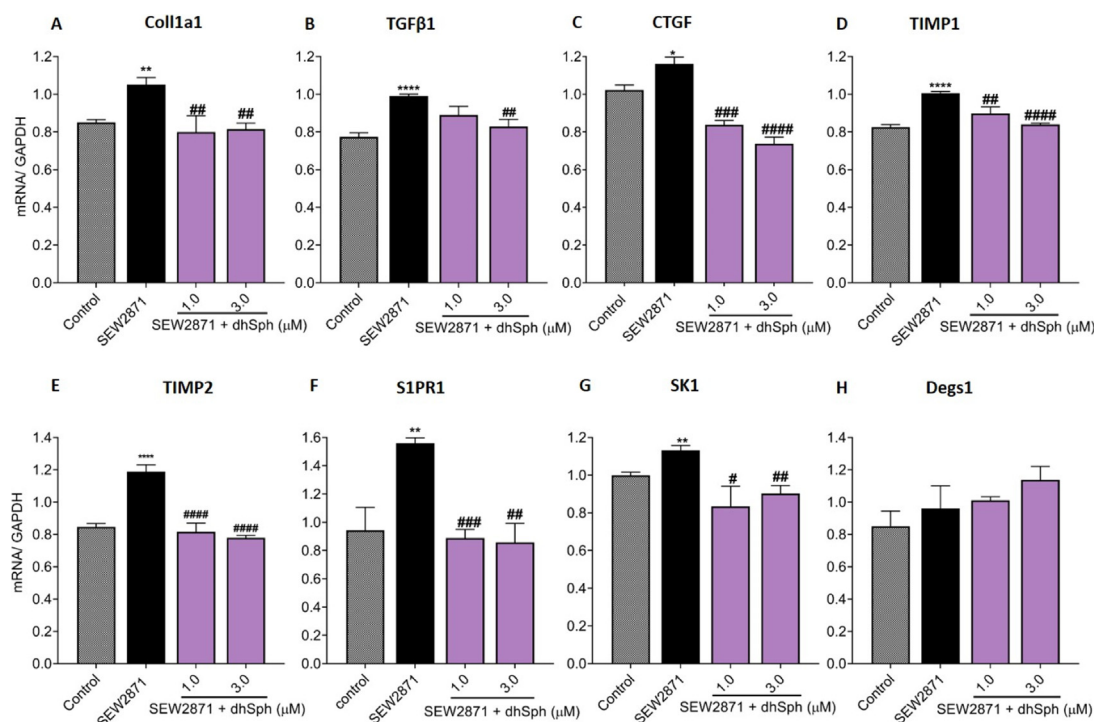


**Fig. 8.** Effects of dhSph on SEW2871 induced fibrotic and sphingolipid related genes. (A–E) DhSph reduced the fibrotic genes; Coll1a1, TGFβ1, CTGF, TIMP1, and TIMP2 mRNA levels elevated by SEW2871, in NCFs treated with SEW2871 (10 μM) for 18 h. (F–G) DhSph also reduced S1PR1 and SK1 mRNA levels. Both SEW2871 and dhSph had no effect on Degs1 gene expression. #####  $p < 0.0001$ , ###  $p < 0.005$ , ##  $p < 0.01$ , #  $p < 0.05$  vs. treatment, and \*\*\*\*  $p < 0.0001$ , \*\*  $p < 0.01$ , \*  $p < 0.05$  vs. control. Data are presented as  $\pm$  SEM of 3 replicates.

acyl chain lengths [19]. This balancing act of increasing short chains with reduced short chains is often observed in studies involving inhibition or knockout of CerS and manifest in different pathologies and their treatment [28,29]. CerS2 increase has been shown to be involved in reduced inflammation in the lung [28], but this cannot be ascertained for our study. Another aspect of this counter balancing act is also known to occur via the Cer/S1P rheostat which determines whether cells survive (S1P) or die through apoptosis (Cer) [30]. The increase and constancy of S1P d18:1 (Fig. 4C2) maybe due to this rheostat, since Cer d18:1/18:0 which has remarkably high basal levels is also increased and drops back to basal levels at 240 min (Fig. 4A2). In contrast, the enrichment of dhS1P and dhCer occurred at around 10 min and stayed elevated for the duration of the study. The increase in dhS1P also exceeded S1P (C16:1) which had a comparatively higher basal level.

The effects of dhSph on Akt could be a result of the increase in Cer [31]. This is highly likely in view of the similarity between Sph and dhSph effect on Akt and RPS6 phosphorylation as shown in Fig. 3C and D. When Sph is incorporated into cells, enrichment of Cer predominates [32]. The downstream Akt target, RPS6, mediates transcription of genes including proliferation, and cell survival [33,34]. TGFβ can activate the PI3K/ Akt signalling and can be dependent or independent of SMADs [35,36]. The addition of dhSph was able to inhibit this signalling interactions. Our findings indicate that the inhibition of collagen synthesis and the TGFβ/ SMAD2 signalling by dhSph seems to be independent of the effects on Akt due to an increase in Cer. Additionally, these inhibitory effects did not involve other downstream non-canonical signalling pathways and molecules such as ERK, P38-MAPK, NF-Kβ and STAT1 (Fig. 3A–B, E–G).

Despite dhS1P being consistently enriched at different time points in this study (Fig. 4B1), and a previous report suggesting anti-fibrotic effects in dermal fibroblasts [37], exogenous dhS1P had a synergistic influence on TGFβ induced collagen synthesis in

NCFs (Fig. 5A). Our previous findings have shown that exogenous dhS1P alone can induce collagen synthesis [14]. Additionally, SK1 preferentially increases dhS1P and not S1P when dhSph is added exogenously [7]. Studies from our group and others have shown that dhS1P and S1P activate signalling pathways through their G protein coupled receptors, S1PRs, and are capable of “inside-out” signalling [14,38]. Therefore, there is a possibility that the increased intracellular dhS1P, via inside out signalling, may have inhibited the TGFβ/SMAD signalling through its effects on phosphatase and tensin homolog (PTEN) as described by Bu and colleagues [39]. Additionally, the immunomodulator, fingolimod (FTY-720), has been shown to increase intracellular dhS1P [40], and was recently demonstrated to reduce existing cardiac hypertrophy and fibrosis in a pressure overload model [41].

Apart from the increased enrichment of dhS1P, exogenous dhSph inhibited collagen synthesis induced by the S1PR1 agonist, SEW2871 (Fig. 5C). This inhibition also led to profound reductions in the transcription levels of known fibrotic markers, such as TGFβ1, Coll1a1, CTGF, TIMP1 and TIMP2 (Fig. 8A–E). Similar effects were observed in TGFβ induced increase in mRNA levels of TGFβ1 and TIMP1 (Fig. 6A), which were reduced by dhSph. There were no changes in these genes in Sph treated cells (Fig. 6B and 7B). Moreover, dhSph affected S1PR1 transcription levels in both TGFβ (Fig. 7A) and SEW2871 (Fig. 8F) treated cells, implying a connection between the receptor and dhSph activated sphingolipid pathway. Unlike S1PR2 and 3, S1PR1 exclusively couples to the G<sub>i</sub> protein to transduce its signals [42]. One of the main downstream pathways that G<sub>i</sub> proteins activate is the PI3K/Akt pathway, however similar inhibitory effects were not observed in cells that had Sph added exogenously. Further examination of dhSph effects on the transcription level of sphingolipid pathway enzymes showed some differences between TGFβ and SEW2871 treated NCFs. TGFβ increased both SK1 and Degs1 mRNA expression (Fig. 7A). The effects of TGFβ on SK1 are known [11], while its effect on Degs1

transcription is a new finding. Exogenous dhSph did not have any effect on SK1 and Degs1 mRNA levels in the presence of TGF $\beta$  and SEW2871, perhaps due to the independent effect of dhSph in the absence of other stimulants (supplementary Fig. 1B). Contrarily, exogenous dhSph reduced SK1 mRNA levels in the presence of SEW2871 (Fig. 8G), indicating that the transcription of SK1 in SEW2871 treated NCFs may depend on S1PR1 activation. TGF $\beta$ 's direct effect on SK1 may have influenced the increased S1PR1 expression by dhSph [11]. There was no effect on Degs1 transcription after dhSph co-treatment in the presence SEW2871 in NCFs (Fig. 8H). The inhibition of collagen synthesis through S1PR1 inhibition by dhSph implies the existence of a negative feedback mechanism employed by the increased dhSph substrate availability on S1PR1. Berdysev and colleagues have alluded to the existence of such a mechanism which they termed the substrate-enzyme-receptor complex [7]. The Des-1 enzyme could be the mediator between dhSph and S1PR1 in this case, as there was no effect on its transcription levels in the presence of either TGF $\beta$  or SEW2871, furthermore it is classically known as the "gate keeper" enzyme in the sphingolipid pathway. It should be noted that inhibiting SK1 and SK2 may not necessarily yield similar results in NCFs to those observed in this study. Together with limitations such the lack of measurement of dhSph-d7 in the media, protein expression of sphingolipid pathway enzymes, CerS1-6 mRNA expression, and non-inclusion of "loss of function" studies, the findings of this study should be regarded as preliminary. See Fig. 9 for summary of findings.

In conclusion, the collagen reducing effects of dhSph in the presence of TGF $\beta$  are associative, and can be attributed to increased sphingolipids, such as dhS1P, in the *de novo* synthetic pathway. This study further highlighted the involvement of sphingolipid metabolic pathway's substrate-enzyme-receptor interactions in

pathological events such as fibrosis, and thus, the need for investigating the effects of intracellularly generated dhS1P.

## Funding

This research was supported by National Health and Medical Research Council of Australia (Program Grants 1092642 and Project Grant 1087355). RM and FS are supported by the Monash University International Post Graduate Research Scholarships and Monash Graduate Scholarships.

## CRediT authorship contribution statement

**Ruth R. Magaye:** Data curation, Methodology, Writing - original draft, Writing - review & editing. **Febby Savira:** Data curation, Writing - original draft. **Xin Xiong:** Data curation, Writing - review & editing. **Kevin Huynh:** Data curation, Writing - review & editing. **Peter J. Meikle:** Data curation, Writing - review & editing. **Christopher Reid:** Writing - review & editing. **Bernard L. Flynn:** Writing - review & editing. **David Kaye:** Writing - review & editing. **Danny Liew:** Writing - review & editing. **Bing H. Wang:** Conceptualization, Methodology, Supervision, Writing - review & editing.

## Declaration of Competing Interest

The authors declare that they have no known competing financial interests or personal relationships that could have appeared to influence the work reported in this paper.

## Acknowledgements

We would like to thank and acknowledge the scientists at the Metabolomics Laboratory- Baker Heart and Diabetes Institute, for conducting the lipidomics analysis described in this study.

## Appendix A. Supplementary material

Supplementary data to this article can be found online at <https://doi.org/10.1016/j.ijcha.2021.100837>.

## References

- [1] R.R. Magaye et al., The role of dihydro sphingolipids in disease, *Cell. Mol. Life Sci.* 76 (6) (2019) 1107–1134.
- [2] Górski, J., et al., Effect of atrial pacing on the level of bioactive sphingolipids in the heart ventricles of the rat. *Atherosclerosis*. 241(1): p. e122–e123.
- [3] L. Sun et al., Comprehensive metabolomic analysis of heart tissue from isoproterenol-induced myocardial infarction rat based on reversed-phase and hydrophilic interaction chromatography coupled to mass spectrometry, *J. Sep. Sci.* 40 (10) (2017) 2198–2206.
- [4] E.E. Egom et al., Serum sphingolipids level as a novel potential marker for early detection of human myocardial ischaemic injury, *Front. Physiol.* 4 (2013) 130.
- [5] M. Knapp et al., Decreased free sphingoid base concentration in the plasma of patients with chronic systolic heart failure, *Adv. Med. Sci.* 57 (1) (2012) 100–105.
- [6] M. Knapp et al., Plasma sphingosine-1-phosphate concentration is reduced in patients with myocardial infarction, *Med. Sci. Monit.* 15 (9) (2009) CR490–3.
- [7] E.V. Berdysev et al., De novo biosynthesis of dihydro sphingosine-1-phosphate by sphingosine kinase 1 in mammalian cells, *Cell. Signal.* 18 (10) (2006) 1779–1792.
- [8] J.M. Kraveka et al., Involvement of dihydroceramide desaturase in cell cycle progression in human neuroblastoma cells, *J. Biol. Chem.* 282 (23) (2007) 16718–16728.
- [9] P. Breen et al., Dihydroceramide Desaturase Knockdown Impacts Sphingolipids and Apoptosis after Photodamage in Human Head and Neck Squamous Carcinoma Cells, *Anticancer Res.* 33 (1) (2013) 77–84.
- [10] W. Ruangsiriluk et al., Silencing of enzymes involved in ceramide biosynthesis causes distinct global alterations of lipid homeostasis and gene expression, *J. Lipid Res.* 53 (8) (2012) 1459–1471.
- [11] F. Cencetti et al., Transforming Growth Factor-1 Induces Transdifferentiation of Myoblasts into Myofibroblasts via Up-Regulation of Sphingosine Kinase-1/S1P3 Axis, *Mol. Biol. Cell* 21 (2010) 1111–1124.

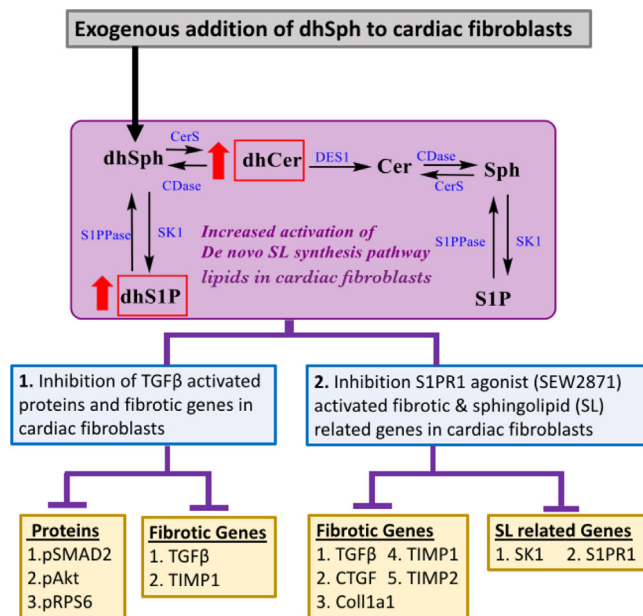


**Fig. 9.** DhSph driven increase in *de novo* sphingolipid synthesis inhibits collagen synthesis in NCFs by TGF $\beta$ . Exogenous dhSph drives the *de novo* sphingolipid synthesis pathway as indicated with the red arrows. DhCer and dhS1P (red squares) were increased the most. The increased activation of the *de novo* pathway was able to 1) inhibit TGF $\beta$  activated pSMAD2 and non-canonical pathway proteins such as pAkt and pRPS6, which also led to reduced expression of fibrotic gene markers such as TGF $\beta$ 1 and TIMP1. (2) DhSph inhibited the S1PR1 agonist, SEW2871, induced collagen synthesis by reducing TGF $\beta$ 1, TIMP1, CTGF, and TIMP2 mRNA expression, perhaps through a substrate-enzyme-receptor interaction. Illustrated using ChemDraw Professional 7.0 (Perkin Elmer, MA, USA).

- [12] S. Lekawanvijit et al., Does indoxyl sulfate, a uraemic toxin, have direct effects on cardiac fibroblasts and myocytes?, *Eur. Heart J.* 31 (14) (2010) 1771–1779.
- [13] P. Simpson, Stimulation of hypertrophy of cultured neonatal rat heart cells through an alpha 1-adrenergic receptor and induction of beating through an alpha 1- and beta 1-adrenergic receptor interaction. Evidence for independent regulation of growth and beating, *Circ. Res.* 56 (6) (1985) 884–894.
- [14] R.R. Magaye et al., Exogenous dihydrosphingosine 1 phosphate mediates collagen synthesis in cardiac fibroblasts through JAK/STAT signalling and regulation of TIMP1, *Cell. Signal.* 72 (2020) 109629.
- [15] K. Huynh et al., High-Throughput Plasma Lipidomics: Detailed Mapping of the Associations with Cardiometabolic Risk Factors, *Cell Chem. Biol.* 26 (1) (2019) 71–84.e4.
- [16] J.M. Weir et al., Plasma lipid profiling in a large population-based cohort, *J. Lipid Res.* 54 (10) (2013) 2898–2908.
- [17] A. Sugiyama et al., Long-term administration of recombinant canstatin prevents adverse cardiac remodeling after myocardial infarction, *Sci. Rep.* 10 (1) (2020) 12881.
- [18] N. Yamashita et al., Intratubular epithelial-mesenchymal transition and tubular atrophy after kidney injury in mice, *American J. Physiol.-Renal Physiol.* 319 (4) (2020) F579–F591.
- [19] M. Levy, A.H. Futerman, Mammalian ceramide synthases, *IUBMB Life* 62 (5) (2010) 347–356.
- [20] B. Ogretmen, Sphingolipid metabolism in cancer signalling and therapy, *Nat. Rev. Cancer* 18 (1) (2018) 33–50.
- [21] A.C. Lewis et al., Targeting sphingolipid metabolism as an approach for combination therapies in haematological malignancies, *Cell Death Discovery* 4 (1) (2018) 72.
- [22] Y.E. Zhang, Non-Smad Signaling Pathways of the TGF- $\beta$  Family, *Cold Spring Harbor Perspect. Biol.* 9 (2) (2017) a022129.
- [23] K. Yamaguchi et al., Identification of a member of the MAPKKK family as a potential mediator of TGF-beta signal transduction, *Science* 270 (5244) (1995) 2008–2011.
- [24] W.-L. Yang et al., The E3 ligase TRAF6 regulates Akt ubiquitination and activation, *Science (New York, N.Y.)* 325 (5944) (2009) 1134–1138.
- [25] R.T. Riley, K.A. Voss, Differential sensitivity of rat kidney and liver to fumonisin toxicity: organ-specific differences in toxin accumulation and sphingoid base metabolism, *Toxicol. Sci.* 92 (1) (2006) 335–345.
- [26] R.T. Riley et al., Evidence for Fumonisin Inhibition of Ceramide Synthase in Humans Consuming Maize-Based Foods and Living in High Exposure Communities in Guatemala, *Mol. Nutr. Food Res.* 59 (11) (2015) 2209–2224.
- [27] K.A. Voss, R.T. Riley, Fumonisin Toxicity and Mechanism of Action: Overview and Current Perspectives, *Food Safety* 1 (1) (2013) 2013006.
- [28] I. Petrache et al., Ceramide Synthases Expression and Role of Ceramide Synthase-2 in the Lung: Insight from Human Lung Cells and Mouse Models, *PLoS ONE* 8 (2013) e62968.
- [29] S. Raichur, Ceramide Synthases Are Attractive Drug Targets for Treating Metabolic Diseases, *Front. Endocrinol.* 11 (483) (2020).
- [30] J.R. Van Brocklyn, J.B. Williams, The control of the balance between ceramide and sphingosine-1-phosphate by sphingosine kinase: Oxidative stress and the seesaw of cell survival and death, *Comp. Biochem. Physiol. B: Biochem. Mol. Biol.* 163 (1) (2012) 26–36.
- [31] K.M. Schubert, M.P. Scheid, V. Duronio, Ceramide Inhibits Protein Kinase B/Akt by Promoting Dephosphorylation of Serine 473, *J. Biol. Chem.* 275 (18) (2000) 13330–13335.
- [32] L. Riboni et al., The Effects of Exogenous Sphingosine on Neuro2a Cells Are Strictly Related to the Overall Capacity of Cells to Metabolize Sphingosine1, *J. Biochem.* 124 (5) (1998) 900–904.
- [33] K.M. Hannan et al., mTOR-Dependent Regulation of Ribosomal Gene Transcription Requires S6K1 and Is Mediated by Phosphorylation of the Carboxy-Terminal Activation Domain of the Nucleolar Transcription Factor UBF $\dagger$ , *Mol. Cell. Biol.* 23 (23) (2003) 8862.
- [34] M.K. Holz et al., mTOR and S6K1 Mediate Assembly of the Translation Preinitiation Complex through Dynamic Protein Interchange and Ordered Phosphorylation Events, *Cell* 123 (4) (2005) 569–580.
- [35] J.Y. Yi, I. Shin, C.L. Arteaga, Type I transforming growth factor beta receptor binds to and activates phosphatidylinositol 3-kinase, *J. Biol. Chem.* 280 (11) (2005) 10870–10876.
- [36] M.C. Wilkes et al., Transforming growth factor-beta activation of phosphatidylinositol 3-kinase is independent of Smad2 and Smad3 and regulates fibroblast responses via p21-activated kinase-2, *Cancer Res.* 65 (22) (2005) 10431–10440.
- [37] S. Bu et al., Dihydrosphingosine-1 phosphate has a potent anti-fibrotic effect in Scleroderma fibroblasts via normalization of PTEN levels, *Arthritis Rheum.* 62 (7) (2010) 2117–2126.
- [38] B.S. Shea, A.M. Tager, Sphingolipid regulation of tissue fibrosis, *Open Rheumatol J* 6 (2012) 123–129.
- [39] S. Bu et al., Opposite effects of dihydrosphingosine 1-phosphate and sphingosine 1-phosphate on transforming growth factor-beta/Smad signaling are mediated through the PTEN/PPM1A-dependent pathway, *J. Biol. Chem.* 283 (28) (2008) 19593–19602.
- [40] E.V. Berdyshev et al., FTY720 Inhibits Ceramide Synthases and Up-regulates Dihydrosphingosine 1-Phosphate Formation in Human Lung Endothelial Cells, *J. Biol. Chem.* 284 (9) (2009) 5467–5477.
- [41] W. Liu et al., A Novel Immunomodulator, FTY-720 Reverses Existing Cardiac Hypertrophy and Fibrosis From Pressure Overload by Targeting NFAT (Nuclear Factor of Activated T-cells) Signaling and Periostin, *Circulation Heart Failure* 6 (4) (2013) 833–844.
- [42] M.J. Lee, M. Evans, T. Hla, The inducible G protein-coupled receptor edg-1 signals via the G(i)/mitogen-activated protein kinase pathway, *J. Biol. Chem.* 271 (19) (1996) 11272–11279.